Breakdown Mechanism of Liquid Nitrogen Viewed from Area and Volume Effects

N. Hayakawa, H. Sakakibara, H. Goshima, M. Hikita and H. Okubo

Nagoya University, Nagoya, Japan

ABSTRACT

We investigated the area and volume effects on the breakdown strength in liquid nitrogen (LN_2) to discuss breakdown mechanism in cryogenic liquids for superconducting power apparatus. We measured breakdown voltages in LN_2 with and without thermal bubbles over a very wide range of the electrode size. Experimental results revealed that breakdown mechanism changed from area dominant to volume effective region at the larger electrode configurations in LN_2. Moreover, we discussed the contribution rate of area and volume effects to the breakdown strength in LN_2. It was suggested that mutual contribution of area and volume effects appeared in breakdown characteristics in LN_2 under thermal bubble condition, as a phenomenon peculiar to cryogenic liquids. Consequently, we pointed out that it is very important to consider both thermal bubbles and electrode surface condition for HV insulation of superconducting power apparatus.

1. INTRODUCTION

SUPERCONDUCTING power transmission technology is one of the most promising candidates for realizing a large power transmission system in the next generation. In order to develop superconducting power apparatus, it is necessary to establish the electrical insulation technique in cryogenic liquids. However, most of the data on electrical insulation at cryogenic temperatures have been obtained under limited experimental conditions; *i.e.* measurements were performed under fundamental experimental conditions to focus mainly on physics. Thus, it is important to obtain data available for practical insulation design of superconducting power apparatus [1–3].

It is well known that the area effect of SF_6 gas and the volume effect of transformer oil have been taken into account statistically for the practical electrical insulation design of gas insulated switchgears (GIS) and power transformers, respectively [4, 5]. However, few attempts have been made until now to design the practical insulation for superconducting power apparatus using cryogenic liquids. From this point of view, we have been investigating the area and volume effects on the breakdown characteristics in cryogenic liquids [6, 7].

In this paper, we discuss the contribution rate of the area effect and the volume effect to the breakdown strength in LN_2. In cryogenic liquids, micro-protrusions on the electrode surface and thermal bubbles in the gap space may be regarded as main weak points for the area effect and the volume effect, respectively. Therefore, we measured the ac breakdown voltage in LN_2 under the combined conditions of thermal bubbles and rough surface electrode. From this investigation, we examined the breakdown mechanism of LN_2 in terms of the mutual correlation of the area and volume effects.

2. EXPERIMENTAL SETUP FOR BREAKDOWN VOLTAGE MEASUREMENT IN LN_2

2.1. ELECTRODE CONFIGURATIONS

Figure 1 shows the electrode configurations for breakdown voltage measurement in LN_2. In order to investigate the area and volume effects over a wide range of the electrode size, we used two kinds of electrode configurations; sphere-to-plane electrode and coaxial cylindrical electrode as shown in Figure 1. For the sphere-to-plane electrode configuration, the highly stressed electrode area (SEA) and liquid volume (SLV) varied with the sphere diameter d and the gap length g. The electrode surface was made to a mirror finish (roughness is < 1 μm).

On the other hand, for the coaxial cylindrical electrode configuration, SEA and SLV varied with the gap length g and the electrode length L. The surface of the inner cylindrical electrode was made either to a mirror finish or a rough finish (roughness is $\sim$ 200 μm). Moreover, a heater was wound around the outer cylindrical electrode so as to generate thermal bubbles in the gap space. The surface of the outer cylinder was made to a mirror finish. These electrode configurations with quasi-uniform electric field distribution (non-uniformity factor: 1.03 to 1.47) allowed SEA and SLV to be varied from 10^0 to 10^5 mm^2 and from 10^{-1} to 10^5 mm^3, respectively. Thus, we can examine the area and volume effects in LN_2 over a very wide variation of the electrode size. All the electrodes were made of stainless steel.

1070–9878/97/$3.00

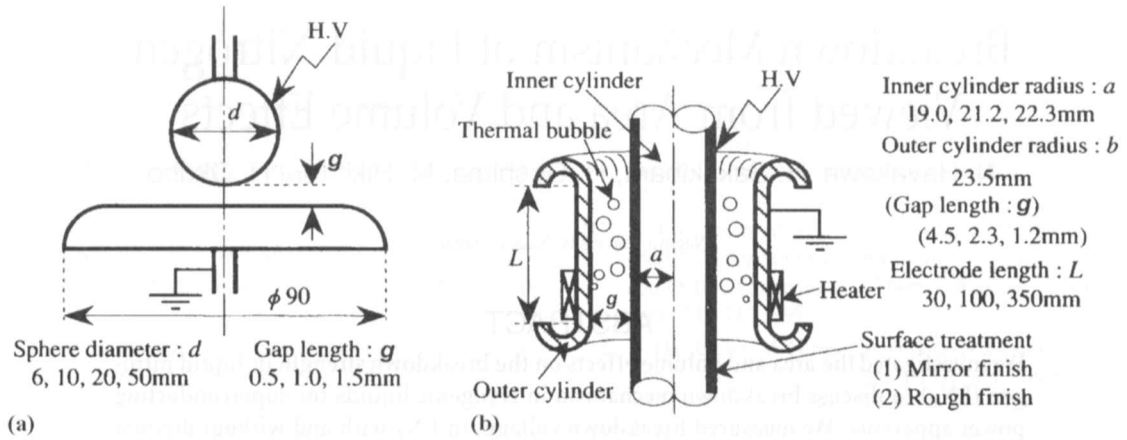

Figure 1. Electrode configurations for breakdown voltage measurement in LN_2. (a) Sphere-to-plane electrode, (b) coaxial cylindrical electrode.

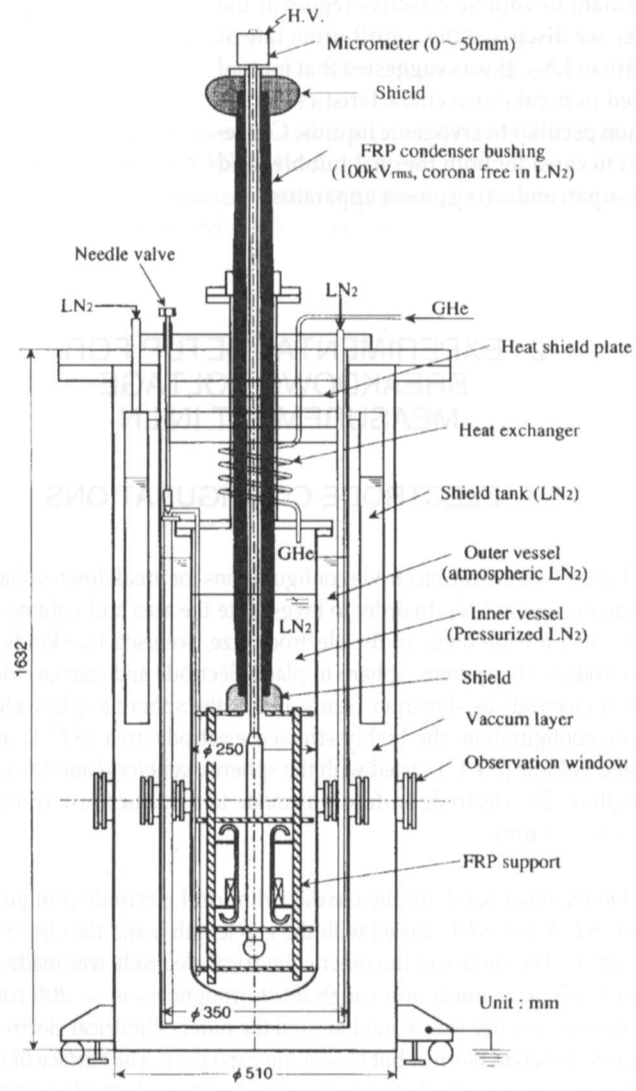

Figure 2. Schematic view of stainless cryostat.

2.2. CRYOSTAT AND EXPERIMENTAL METHOD

In our experiments, we used two kinds of cryostats; fiber reinforced plastic (FRP) cryostat and stainless cryostat. FRP cryostat composed of LN_2 vessel and vacuum layer was used for measuring the breakdown characteristics of LN_2 at the atmospheric pressure with thermal bubbles generated by a heater. On the other hand, a stainless cryostat was used for pressurized LN_2. Figure 2 shows a schematic view of the stainless cryostat. It was composed of four elements; LN_2 shield tank, vacuum layer, LN_2 outer vessel (LN_2 at the atmospheric pressure) and LN_2 inner vessel (pressurized LN_2). Observation windows were also installed in four directions to observe thermal bubble behavior, discharges and so on in LN_2. An FRP condenser bushing with 100 kV_{rms} corona free ability in LN_2 was mounted on the stainless cryostat. In our experiments, LN_2 was pressurized with gaseous helium at the pressure from 0.1 to 0.5 MPa, so that thermal bubbles could be suppressed in subcooled LN_2 at 77 K.

Testing electrodes were placed vertically, as shown in Figure 1, either in FRP or stainless cryostat, and immersed in LN_2. High ac voltage with the frequency of 60 Hz was applied to the sphere or the inner cylindrical electrode at a rising rate of 5 kV_{rms}/s. Under these conditions, we performed breakdown tests 50 times for each experimental setup as parameters of electrode size, electrode surface condition, heater power and pressure.

3. BREAKDOWN CHARACTERISTICS IN LN_2 UNDER THERMAL BUBBLE CONDITION

3.1. AREA AND VOLUME EFFECTS ON BREAKDOWN STRENGTH IN LN_2 AT THE ATMOSPHERIC PRESSURE

Figures 3(a) and (b) show the area and volume effects on ac breakdown strength in LN_2 at the atmospheric pressure [6]. SEA and SLV are defined as electrode surface area and liquid volume, respectively, with the electric field strength beyond 82% of the maximum strength [7]. In these Figures, we introduced other researchers' data [6] into our study and systematized the area and volume effects in LN_2. It is found that breakdown strength in LN_2 linearly decreases with increasing SEA and SLV in the log – log scale over 5 to

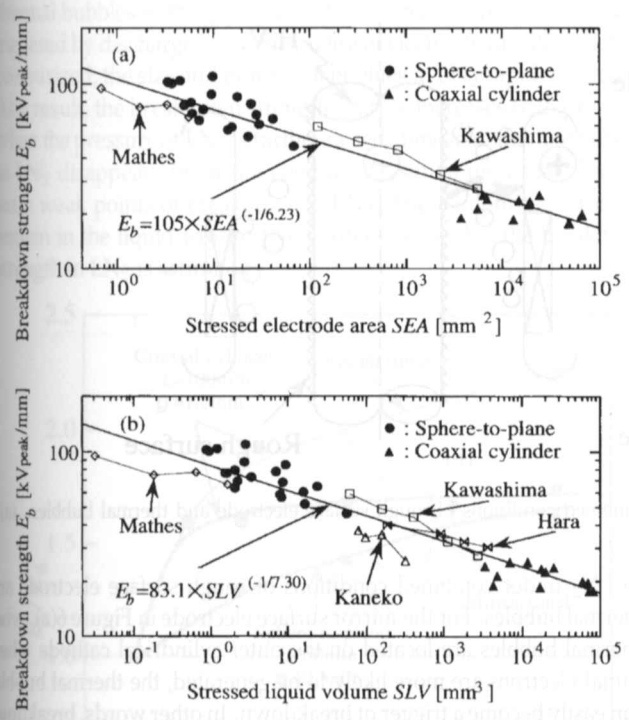

Figure 3. Area effect and volume effect on ac breakdown strength in LN_2 at the atmospheric pressure [6], (a) area effect, (b) volume effect.

6 orders of SEA and SLV. These results indicate that the insulation characteristics of LN_2 largely depend on the stressed area and volume.

In Figure 3, the breakdown strength in LN_2 was evaluated as a function of SEA and SLV. It is important for practical insulation design using LN_2 to elucidate the individual contribution of area and volume effects in LN_2; in other words, which effect is more dominant in LN_2. The experiments were performed in the following Sections to answer the above question.

3.2. INFLUENCE OF THERMAL BUBBLES AND ELECTRODE SURFACE CONDITION

Figure 4 shows the ac breakdown voltage U_b in LN_2 at the atmospheric pressure for different electrode surface conditions as a function of the thermal bubble volume V_{Bub} generated by the heater. It is seen that for both mirror and rough finish electrode, U_b sharply decreases with increasing V_{Bub}, and is saturated at the larger V_{Bub}. U_b for the rough finish electrode is slightly smaller than that for the mirror finish electrode. Thus, both thermal bubbles and electrode surface conditions simultaneously affect the breakdown voltage in LN_2.

3.3. MUTUAL CONTRIBUTION OF AREA EFFECT AND VOLUME EFFECT

Figure 5 shows the probability P_r that the breakdown occurs at positive or negative half cycle of the applied ac voltage to the inner cylinder for different bubble volume V_{Bub}. In case of V_{Bub} = 0 cm^3/s, the breakdown probability $P_{r(-)}$ at negative half cycle is

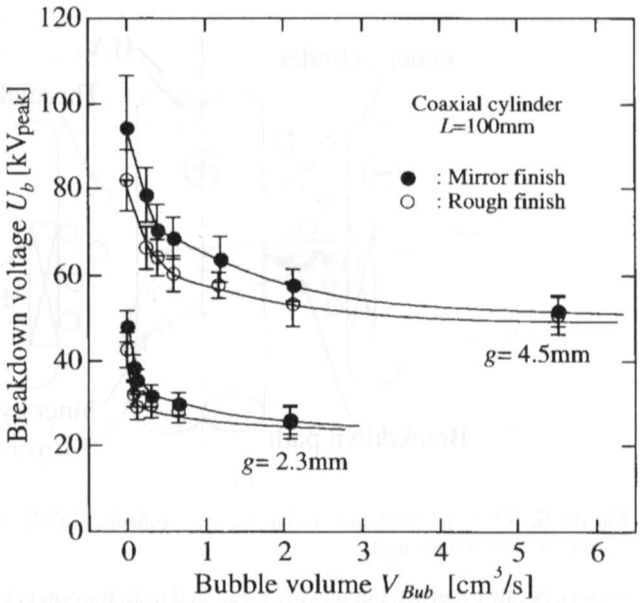

Figure 4. ac breakdown voltage U_b as a function of bubble volume V_{Bub} for different electrode surface conditions.

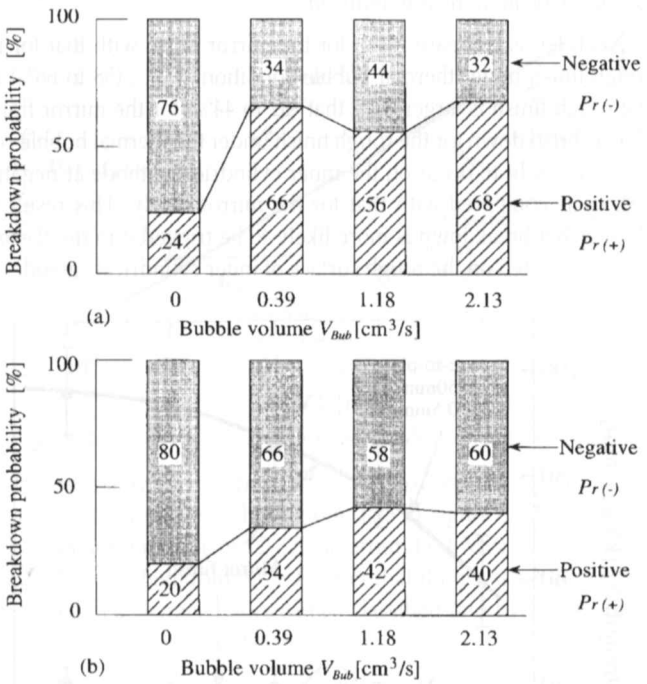

Figure 5. Breakdown probability P_r at positive or negative half cycle of applied ac voltage for different bubble volume V_{Bub}. (Coaxial cylinder: L = 100 mm, g = 4.5 mm) (a) Mirror finish, (b) rough finish.

76% for mirror finish and 80% for the rough finish, being larger than $P_{r(+)}$ at positive half cycle. This result indicates that the breakdown is more likely to be triggered on the inner cylindrical cathode with higher electric field strength by generating initial electrons for a breakdown event. On the other hand, when the thermal bubbles are generated, *i.e.* as V_{Bub} increases, $P_{r(+)}$ becomes larger than $P_{r(-)}$ for the mirror finish as shown in Figure 5(a). The thermal bubbles may be distributed mainly in the vicinity of the ground electrode side (outer

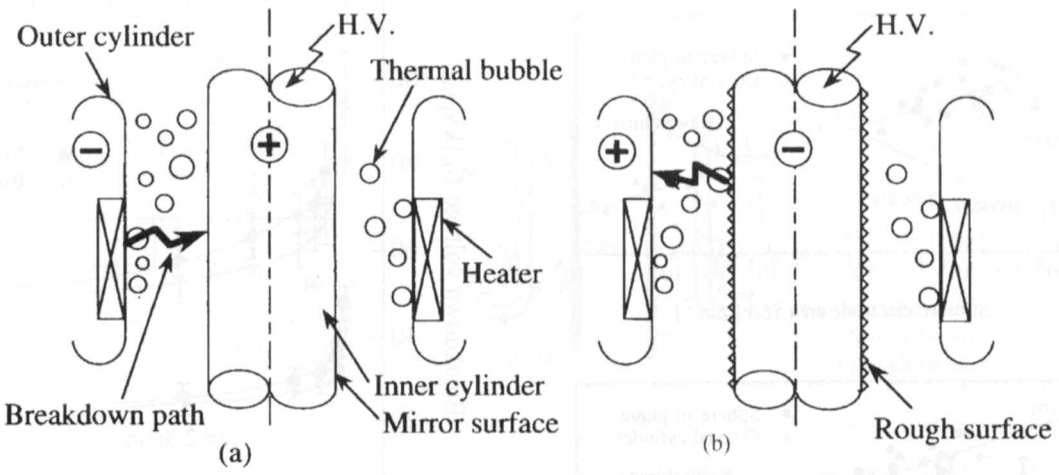

Figure 6. Schematic illustration of breakdown mechanism in LN_2 under combined conditions of rough surface electrode and thermal bubbles. (a) Mirror finish, (b) rough finish.

cylinder), because thermal bubbles are generated from the outer cylinder installing the heater. Thus, when the ground electrode is cathode under the thermal bubble condition, *i.e.* at positive half cycle, breakdown can be more readily induced.

Next, let us compare $P_{r(-)}$ for the mirror finish with that for the rough finish under thermal bubble condition; $P_{r(-)}$ (58 to 66%) for the rough finish is larger than that (32 to 44%) for the mirror finish. Hence, breakdown for the rough finish under the thermal bubble condition is likely to occur on the inner cylindrical cathode at negative half cycle compared with that for the mirror finish. This result indicates that breakdown is more likely to be triggered in the thermal bubbles located on the rough surface of inner cylindrical cathode.

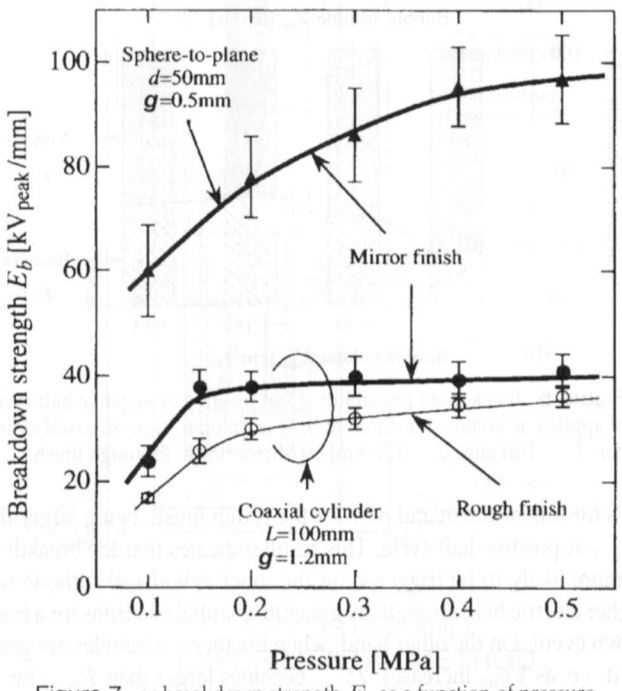

Figure 7. ac breakdown strength E_b as a function of pressure.

Figure 6 shows a schematic illustration of breakdown mechanism in LN_2 under combined conditions of rough surface electrode and thermal bubbles. For the mirror surface electrode in Figure 6(a), when thermal bubbles are located on the outer cylindrical cathode where initial electrons are more likely to be generated, the thermal bubbles can easily become a trigger of breakdown. In other words, breakdown in LN_2 can be triggered by breakdown in thermal bubbles due to their low withstand level. In case of the rough surface on the inner cylindrical cathode in Figure 6(b), the electric field enhancement due to micro-protrusions causes breakdown in thermal bubbles. The above explanation under the thermal bubble condition suggests that breakdown in LN_2 is primarily determined by the volume effect of thermal bubbles, while it is mutually affected by the area effect of rough surface electrode. Consequently, the mutual correlation between the area effect and the volume effect is expected to appear on the breakdown strength in LN_2.

4. BREAKDOWN CHARACTERISTICS IN PRESSURIZED LN_2

4.1. BREAKDOWN STRENGTH IN PRESSURIZED LN_2

Figure 7 shows the ac breakdown strength E_b in LN_2 for sphere-to-plane electrode and coaxial cylindrical electrode as a function of pressure. Moreover, Figure 8 shows the normalized ac breakdown strength E_b/E_0 as a function of pressure. Let E_0 be defined as the breakdown strength at 0.1 MPa. In Figure 7, breakdown strength at 0.1 MPa for coaxial cylinder is smaller than that for sphere-to-plane. The result is attributed to the area and volume effects; coaxial cylindrical electrodes have larger SEA and SLV by the order of three than those for sphere-to-plane electrode, as shown in Figure 3.

It is obvious in Figures 7 and 8 that the breakdown strength of the mirror finish for coaxial cylindrical electrode sharply rises with increasing pressure from 0.1 to 0.15 MPa, and is saturated from 0.15 to 0.5 MPa. These characteristics can be explained as follows. Since the coaxial cylindrical electrode has large SLV, there exists a lot of

thermal bubbles in the gap space. Hence, breakdown in LN_2 may be triggered by discharge in bubbles at lower electric fields. When LN_2 is pressurized, the size and number of bubbles in LN_2 rapidly decrease. As a result, the breakdown strength sharply increases with pressure. When the pressure of LN_2 is further raised, almost all thermal bubbles in LN_2 disappear. In such a condition, residual impurities become main weak points of breakdown in LN_2. These impurities probably remain in the liquid irrespective of pressure, so that the breakdown strength in LN_2 is saturated.

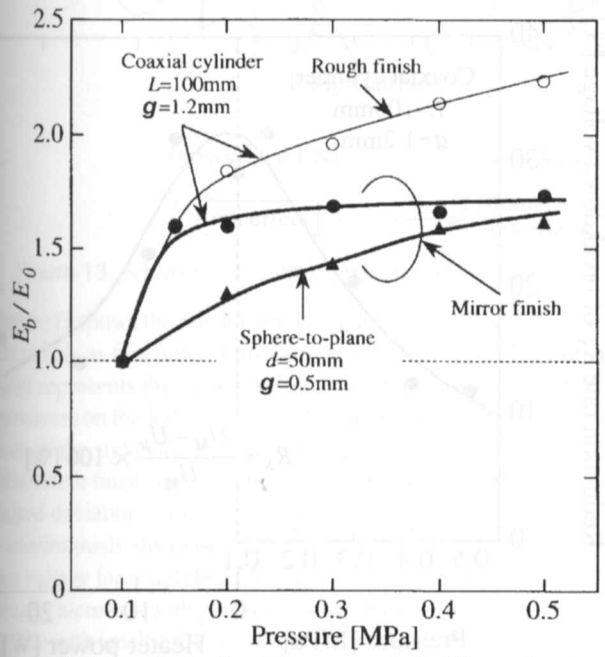

Figure 8. Normalized ac breakdown strength E_b/E_0 as a function of pressure.

On the other hand, it is clear that the breakdown strength for sphere-to-plane electrode gradually increases with pressure. For sphere-to-plane electrode with small SLV, thermal bubbles in gap space cannot become main weak points of breakdown. Hence, breakdown may be triggered under higher electric field by discharge in small bubbles generated from micro-protrusions which enhance the local electric field strength on the electrode surface [8]. When LN_2 is pressurized, the bubbles from the micro-protrusions are kept to be generated with small size in the pressurized LN_2. As a result, the breakdown strength in LN_2 is not saturated but gradually increases with pressure.

4.2. PRESSURE DEPENDENCE OF BREAKDOWN CHARACTERISTICS FROM THE VIEWPOINT OF VOLUME EFFECT

In this Section, we introduced other researchers' data [9–12] on the pressure dependence of breakdown characteristics in LN_2 into our study and verified the breakdown mechanism from the viewpoint of area and volume effects. Table 1 shows their experimental conditions for measurement of ac breakdown strength in pressurized LN_2. In Table 1, we calculated SLV for other researchers' electrode configuration using charge simulation method.

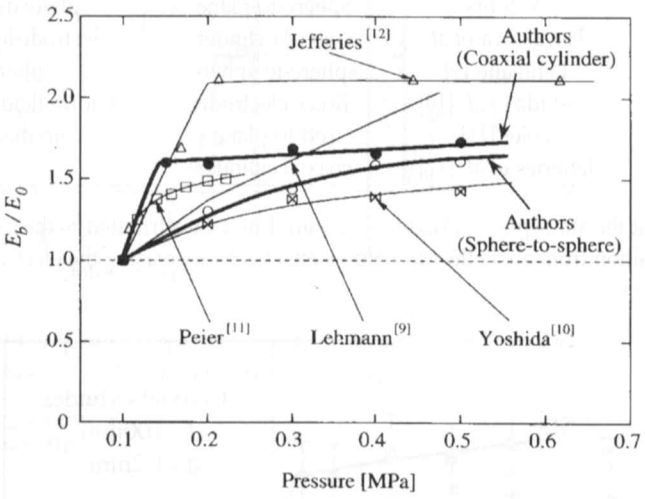

Figure 9. Normalized ac breakdown strength E_b/E_0 as a function of pressure.

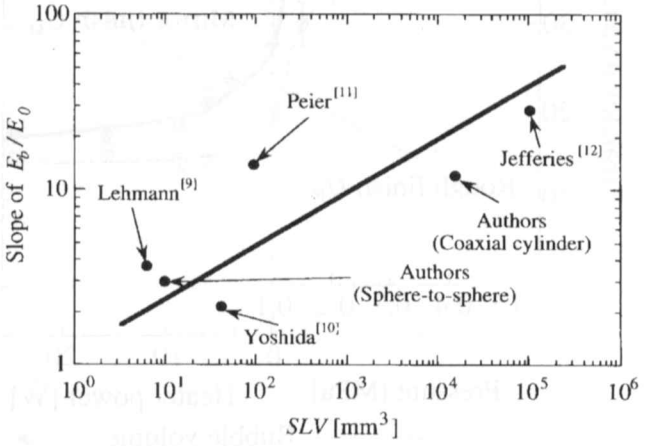

Figure 10. Slope of E_b/E_0 at around 0.1 MPa as a function of SLV.

Figure 9 shows the normalized ac breakdown strength E_b/E_0 as a function of pressure, including our data in Figure 8. Moreover, Figure 10 shows the slope of E_b/E_0 at around 0.1 MPa as a function of SLV. It is verified from these Figures that the pressure dependence of breakdown characteristics can be classified into two categories as described in the previous Section:

1. Breakdown strength for electrodes with large SLV sharply increases at lower pressure and is saturated at higher pressure,
2. Breakdown strength for electrodes with small SLV gradually increases with increasing pressure.

Let us remember the discussion on breakdown mechanism in the previous Section, then it is considered that the former characteristics (1) are mainly derived from the volume effect due to thermal bubbles and residual impurities in the gap space, while the latter characteristics (2) correspond to the area effect due to micro-protrusions on the electrode surface. Thus, it is elucidated how the weak points such as thermal bubbles and micro-protrusions affect the breakdown characteristics in LN_2. From these points of view, the breakdown characteristics in LN_2

Table 1. Experimental conditions for measurement of ac breakdown strength in pressurized LN_2.

Researchers	Electrode configuration	Electrode size	E_0 [kV_{peak}/mm]	SLV [mm^3]
Authors	Sphere-to-plane	sphere diam. 50 mm, gap length 0.5 mm	60.1	9.6
Hayakawa *et al.*	coaxial cylinder	electrode length 100 mm, gap length 1.2 mm	23.7	1.54×10^4
Lehmann [9]	sphere-to-sphere	sphere diam. 62.5, gap length 0.5	44.5	6.0
Yoshida *et al.* [10]	Bruce electrode	uniform field area 160 mm^2, gap length 0.25 mm	41.2	40
Peier [11]	rod-to-plane	tip diam 30 mm, gap length 4.0 mm	50.2	93
Jefferies *et al.* [12]	coaxial cylinder	gap length 6.25 mm	11.2	10^5

at the atmospheric pressure in Figure 1 may be attributed to the transition from area effect to volume effect with increasing the electrode size.

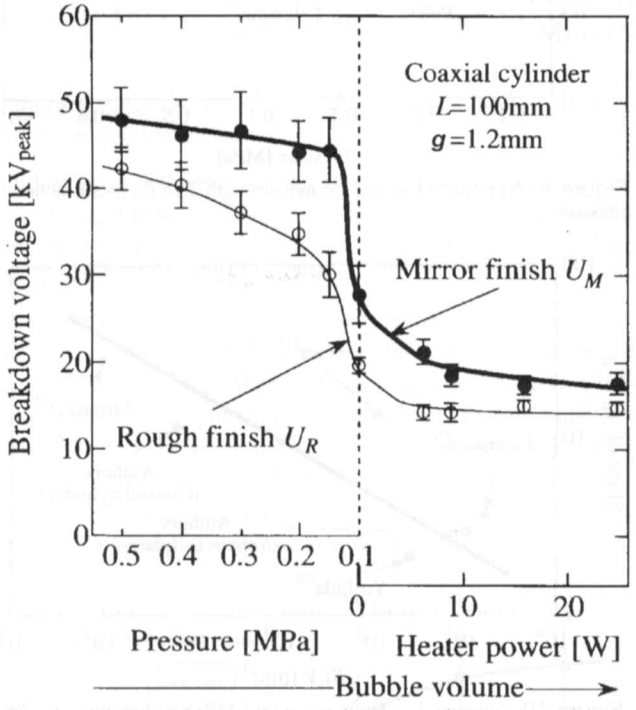

Figure 11. Breakdown voltage as functions of pressure and heater power.

4.3. INFLUENCE OF ELECTRODE SURFACE CONDITION

In this Section, we discuss the influence of electrode surface condition on the pressure dependence of breakdown strength. It is obvious in Figure 7 that in case of coaxial cylinder, breakdown strength for rough finish is slightly smaller than that for mirror finish as in Figure 4. Moreover, it is seen in Figure 8 that for pressure from 0.1 to 0.15 MPa, the slope of E_b/E_0 of coaxial cylinder for rough finish agrees with that for mirror finish. While, for pressure from 0.15 to 0.5 MPa, the slope for coaxial cylindrical electrode for rough finish is nearly equal to that for sphere-to-plane electrode. We interpreted these results as follows. From 0.1 to 0.15 MPa, breakdown for coaxial cylindrical electrode with rough surface may be triggered by thermal bubbles in the gap space with large SLV as seen in Sections 4.1 and 4.2. On the other hand, microscopic electric field strength on the inner

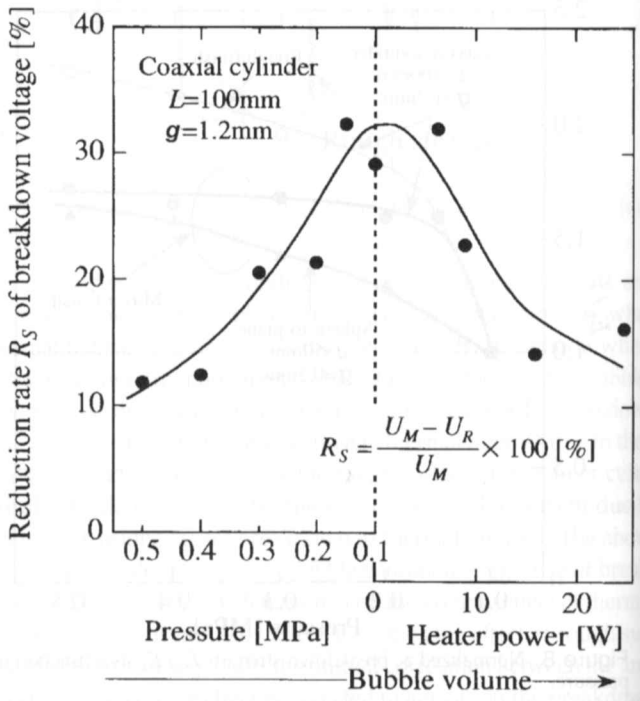

Figure 12. Reduction rate R_S of breakdown voltage under rough surface condition as functions of pressure and heater power.

cylinder with rough surface is enhanced by micro-protrusions. Therefore, from 0.15 to 0.5 MPa, breakdown mechanism for coaxial cylindrical electrode with rough surface may be similar to that for sphere-to-plane electrode, where breakdown was triggered by the thermal bubbles generated by the micro-protrusions.

5. EVALUATION OF MUTUAL CONTRIBUTION OF AREA AND VOLUME EFFECTS

In Section 3, we found that the mutual contribution of the area effect and the volume effect appeared in breakdown characteristics in LN_2 at 0.1 MPa under combined conditions of rough surface and thermal bubbles. The thermal bubbles were generated by the heater in LN_2. On the contrary, in Section 4, the bubbles were suppressed in pressurized LN_2. In this Section, to discuss the mutual contribution of area and volume effects, we combine both data shown in Sections 3 and 4 from the comprehensive viewpoint of bubble volume.

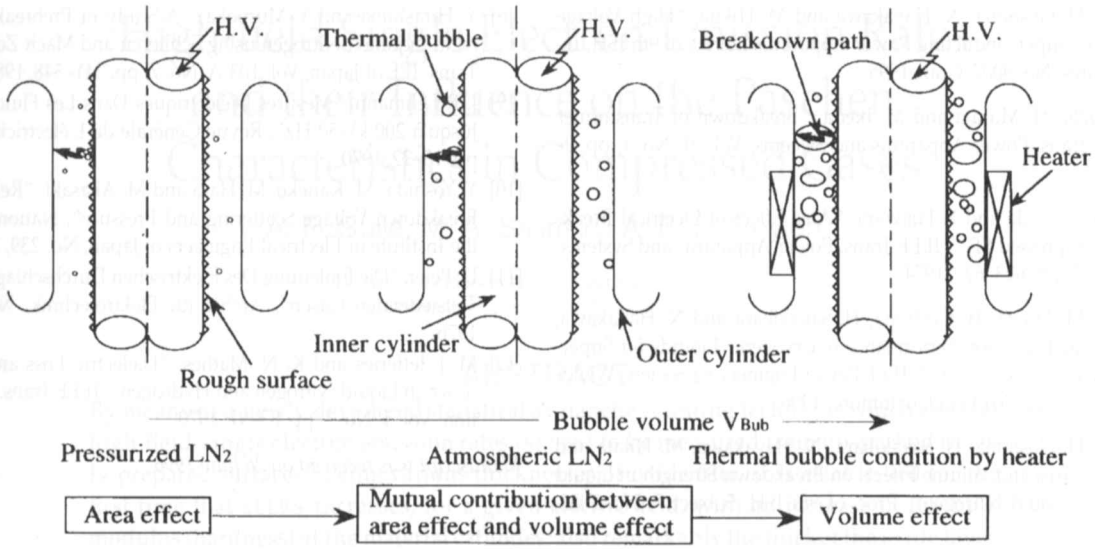

Figure 13. Schematic illustration of transition of breakdown mechanism in LN_2 with increasing bubble volume under rough surface condition.

Figure 11 shows the breakdown voltage for coaxial cylindrical electrode in LN_2 as functions of pressure and heater power. The horizontal axis represents the bubble volume which decreases with increasing pressure on the left side axis and increases with raising the heater power on the right side axis. In this Figure, breakdown voltage U_M for the mirror finish and U_R for the rough finish are plotted with their standard deviation expressed by bars. It is obvious that both U_M and U_R continuously decrease as the bubble volume increases. Breakdown voltage for rough finish is lower than that for mirror finish and gradually increases with pressure, as was the case for sphere-to-plane electrode with small SLV shown in Figures 7 and 8. This is interpreted in terms of the event that the area effect becomes dominant over the volume effect, because the contribution of micro-protrusions on the electrode surface to the breakdown was enhanced by the rough surface. Thus, the rough surface also contributes to the pressure dependence of breakdown characteristics even for the coaxial cylindrical electrode with large SLV, which means that the mutual contribution of area and volume effects definitely appears.

In order to discuss the mutual contribution of area and volume effects, we introduce reduction rate R_S of the breakdown voltage for rough surface conditions to that for mirror surfaces as expressed by

$$R_S = \frac{U_M - U_R}{U_M} \times 100 \qquad (1)$$

In other words, R_S is regarded as a parameter to quantify the effect of surface condition under thermal bubble condition. Figure 12 shows the reduction rate R_S as functions of pressure and heater power. It is found that R_S has a maximum value at $\sim$ 0.1 MPa. This fact shows that the rough surface contributes to the reduction of breakdown voltage in LN_2 in the most effective way at the atmospheric pressure under the thermal bubble condition.

Figure 13 shows a schematic illustration of transition of breakdown mechanism in LN_2 with increasing bubble volume under rough surface condition. When the thermal bubbles increase, the gap space may be filled with bubbles, resulting in higher contribution of the volume effect. On the other hand, when thermal bubbles are suppressed, the area effect may be dominant over the volume effect even for large SLV. Consequently, the area effect mutually contributes to the breakdown characteristics in LN_2 together with the volume effect under thermal bubble condition at $\sim$ 0.1 MPa. Thermal bubbles in LN_2 at the atmospheric pressure are mainly derived from the thermal invasion from the room temperature environment because of much lower latent heat of LN_2 compared with that of transformer oil. Therefore, it is concluded that the mutual contribution of area and volume effects on breakdown strength in LN_2 is peculiar to cryogenic liquids for superconducting power apparatus.

6. CONCLUSIONS

In this paper, we investigated ac breakdown characteristics in LN_2 for practical insulation design of superconducting power apparatus. We discussed breakdown mechanism in LN_2 from the viewpoint of area and volume effects and derived the following results:

1. Volume effect due to thermal bubbles dominated the breakdown strength for electrodes with large SLV.
2. Area effect due to micro-protrusions on the electrode surface appeared for electrodes with small SLV or rough surface.
3. Under the thermal bubble condition, the area and volume effects mutually contributed to the breakdown strength in LN_2.
4. Mutual contribution of area and volume effects was the largest in LN_2 at the atmospheric pressure.

We pointed out that the above breakdown phenomena were peculiar to cryogenic liquids being likely to generate thermal bubbles.

REFERENCES

[1] E. B. Forsyth, "The High Voltage Design of Superconducting Power Transmission Systems", IEEE Electrical Insulation Magazine, Vol. 6, no. 4, pp. 7–16, 1990.

[2] J. Gerhold and M. Hara, "Procedure of Electrical Insulation Design for Superconducting Coils", Proc. of 8th ISH, 93. 04, pp. 567–570, Yokohama, 1993.

[3] H. Okubo, H. Goshima, N. Hayakawa and M. Hikita, "High Voltage Insulation of Superconducting Power Apparatus", Proc. of 9th ISH, Invited Lectures, No. 9007, Graz, 1995.

[4] Y. Kawaguchi, H. Murata and M. Ikeda, "Breakdown of Transformer Oil", IEEE Trans. Power Apparatus and Systems, Vol. 91, No. 1, pp. 9–23, 1972.

[5] T. Nitta, N. Yamada and Y. Fujiwara, "Area Effect of Electrical Breakdown in Compressed SF_6", IEEE Trans. Power Apparatus and Systems, Vol. 93, No. 2, pp. 623–629, 1974.

[6] H. Okubo, M. Hikita, H. Goshima, H. Sakakibara and N. Hayakawa, "High Voltage Insulation Performance of Cryogenic Liquids for Superconducting Power Apparatus", IEEE Power Engineering Society, Winter Meeting, 96WM222-0 PWRD, Baltimore, 1996.

[7] H. Okubo, H. Goshima, H. Sakakibara, N. Hayakawa, M. Hikita and K. Uchida, "Area and Volume Effects on Breakdown Strength in Liquid Helium and Liquid Nitrogen", Proc. of 9th ISH, Subject 7, No. 7052, Graz, 1995.

[8] Y. Hirashima and Y. Murooka, "A Study of Prebreakdown Phenomena in Liquified Nitrogen using Schlieren and Mach Zehnder Methods", Trans. IEE of Japan, Vol. 103-A, No. 7, pp. 341–348, 1983.

[9] J.-P. Lehmann, "Mesures Diélectriques Dans Les Fluides Cryogéniques Jusqu'à 200 kV-50 Hz", Revue Générale de L'électricité, Vol. 79, No. 1, pp. 15–22, 1970.

[10] Y. Yoshida, M. Kaneko, M. Hara and M. Akasaki, "Relation between ac Breakdown Voltage Scattering and Pressure", National Convention of the Institute of Electrical Engineers of Japan, No. 239, 1982.

[11] D. Peier, "Die Einleitung Des Elektrischen Durchschlags in Verflüssigten Tiefsiedenden Gasen", Archiv für Elektrotechnik, No. 58, pp. 39–46, 1976.

[12] M. J. Jefferies and K. N. Mathes, "Dielectric Loss and Voltage Breakdown in Liquid Nitrogen and Hydrogen", IEEE Trans. Electrical Insulation, Vol. 5, No. 3, pp. 83–91, 1970.

Manuscript was received on 26 June 1996.